Title

Expression, purification and preliminary crystallographic analysis of Mycobacterium tuberculosis CysQ, a phosphatase involved in sulfur metabolism.

Journal

Acta crystallographica. Section F, Structural biology communications, 70(Pt 6)

ISSN

2053-230X

Authors

Erickson, Anna I
Sarsam, Reta D
Fisher, Andrew J

Publication Date

2014-06-10

Peer reviewed

Acta Crystallographica Section F
Structural Biology Communications
ISSN 2053-230X

Expression, purification and preliminary crystallographic analysis of *Mycobacterium tuberculosis* CysQ, a phosphatase involved in sulfur metabolism

Anna I. Erickson, Reta D. Sarsam and Andrew J. Fisher

Acta Cryst. (2014). F**70**, 750–753

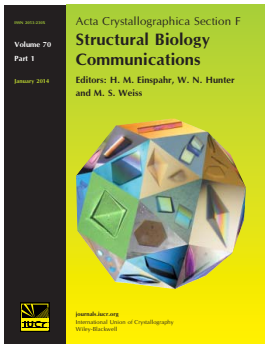

Acta Crystallographica Section F
Structural Biology Communications
ISSN 2053-230X

Expression, purification and preliminary crystallographic analysis of *Mycobacterium tuberculosis* CysQ, a phosphatase involved in sulfur metabolism

Anna I. Erickson,[a] Reta D. Sarsam[b] and Andrew J. Fisher[a,b,c]*

[a]Graduate Program in Biochemistry, Molecular, Cellular and Developmental Biology, University of California, One Shields Avenue, Davis, CA 95616, USA, [b]Department of Molecular and Cellular Biology, University of California, One Shields Avenue, Davis, CA 95616, USA, and [c]Department of Chemistry, University of California, One Shields Avenue, Davis, CA 95616, USA

Correspondence e-mail: ajfisher@ucdavis.edu

Received 27 February 2014
Accepted 16 April 2014

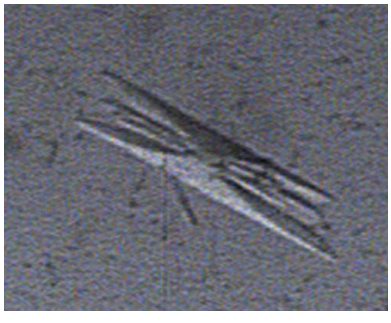

CysQ is part of the sulfur-activation pathway that dephosphorylates 3′-phosphoadenosine 5′-monophosphate (PAP) to regenerate adenosine 5′-monophosphate (AMP) and free phosphate. PAP is the product of sulfate-transfer reactions from sulfotransferases that use the universal sulfate donor 3′-phosphoadenosine 5′-phosphosulfate (PAPS). In some organisms PAP is also the product of PAPS reductases that reduce sulfate from PAPS to sulfite. CysQ from *Mycobacterium tuberculosis*, which plays an important role in the biosynthesis of sulfated glycoconjugates, was successfully purified and crystallized in 24% PEG 1500, 20% glycerol. X-ray diffraction data were collected to 1.7 Å resolution using a synchrotron-radiation source. Crystals grew in the orthorhombic space group $P2_12_12_1$, with unit-cell parameters a = 40.3, b = 57.9, c = 101.7 Å and with one monomer per asymmetric unit.

1. Introduction

Mycobacterium tuberculosis is the causative agent of most cases of tuberculosis (TB), which kills approximately 1.6 million people each year, making it a global health issue. The World Health Organization estimated 8.6 million new cases of *M. tuberculosis* infection in 2012 (World Health Organization, 2013). Multidrug-resistant (MDR) strains are appearing in 3.6% of new cases and compose an estimated 20% of previously treated cases (World Health Organization, 2013). MDR-TB is a strain resistant to the two most commonly used first-line drug treatments, isoniazid and rifampin. In 2008, 46 countries reported cases of extensively drug-resistant (XDR) TB, which is resistant to isoniazid, rifampin, fluoroquinolone derivatives and at least one of three available injectable second-line drugs (Fauci, 2008; World Health Organization, 2013). XDR-TB is predicted to cover 9.6% of reported MDR-TB cases (World Health Organization, 2013).

The increasing prevalence of drug-resistant strains of *M. tuberculosis* presents a global need for novel antibiotics (Fauci, 2008; World Health Organization, 2013). Recent research efforts have found that genes involved in sulfur metabolism are up-regulated and critical for the persistent stage of infection, and these gene products may present novel bacteria-specific targets for drug discovery (Paritala & Carroll, 2013; Pinto *et al.*, 2004; Sassetti *et al.*, 2001, 2003). The sulfate-activation pathway converts relatively inert sulfate into the sulfur-containing metabolites found in the cell. The first enzyme in the pathway, ATP sulfurylase (CysD), catalyzes the adenylyl transfer of ATP to sulfate to generate adenosine 5′-phosphosulfate (APS) and pyrophosphate (Fig. 1). APS can be either directly reduced to sulfite by the enzyme APS reductase (CysH) or phosphorylated to form the universal sulfate donor 3′-phosphoadenosine 5′-phosphosulfate (PAPS; Sekowska *et al.*, 2000). The phosphorylation of APS is carried out by the APS kinase domain (CysC) of the CysNC bifunctional enzyme (Pinto *et al.*, 2004). The sulfotransferases use PAPS as a sulfate donor to generate a wide array of sulfate-containing metabolites (Mougous *et al.*, 2002). The remaining product molecule of the sulfotransferases, 3′-phosphoadenosine 5′-monophosphate (PAP), is a competitive inhibitor of some sulfotransferases (Paritala & Carroll, 2013; Pi *et al.*, 2005). Therefore, PAP is depleted in the cell through the activity of 3′-phosphoadenosine-5′-phosphatase (CysQ), which converts PAP to AMP (adenosine 5′-monophosphate) and inorganic phosphate (Fig. 1).

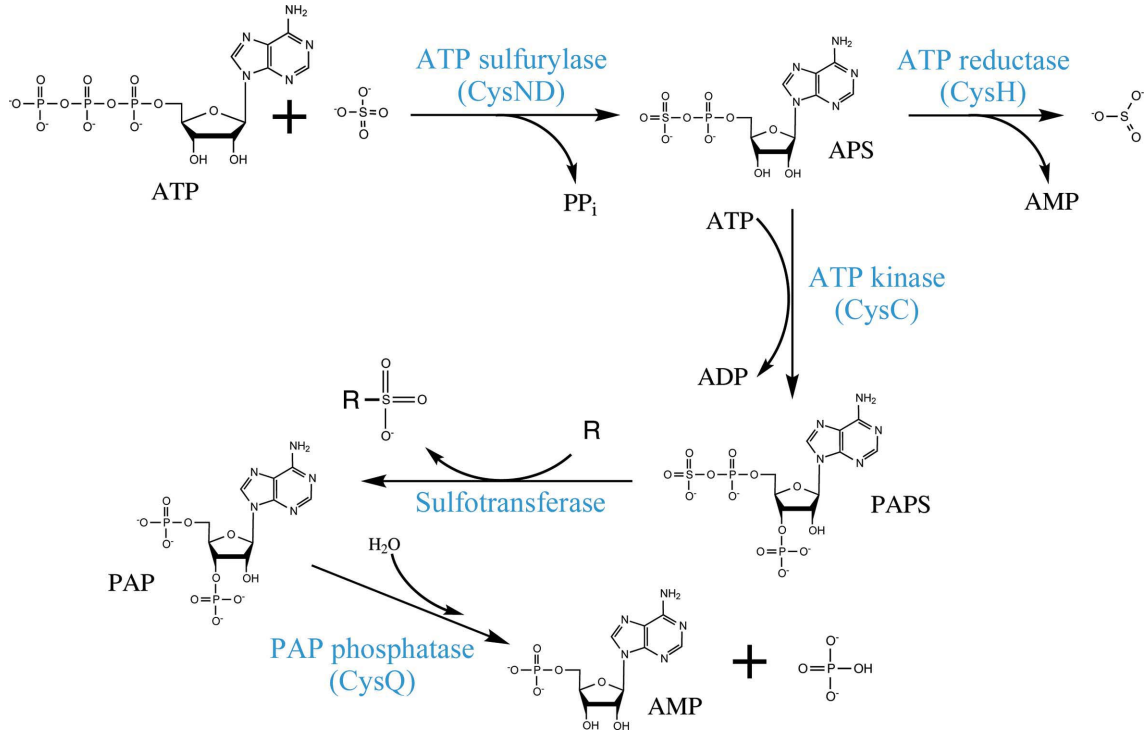

Figure 1
The *M. tuberculosis* sulfur-activation pathway showing product molecules from the reduction and sulfur-transfer reactions. Gene-product names for the enzymes are indicated in parentheses.

Hatzios *et al.* (2008) identified the *M. tuberculosis* gene *Rv2131c* as the enzyme CysQ, a PAP phosphatase. The same laboratory also found that TB strains with a deleted *cysQ* gene had reduced quantities of sulfated glycolipids (Hatzios *et al.*, 2011). Specifically, they found that sulfolipid-1 levels were reduced to a third of the wild-type levels. Sulfolipid-1 has been implicated in the virulence of *M. tuberculosis* (Goren *et al.*, 1974). To gain insight into structure–function activity relationships of this important enzyme, we report here the cloning, overexpression, purification and crystallization of CysQ from *M. tuberculosis*.

2. Materials and methods

2.1. Cloning

The *cysQ* gene (*Rv2131c*) was PCR-amplified from *M. tuberculosis* H37Rv genomic DNA. The primers contained *Nde*I and *Xho*I restriction sites for insertion into the expression vector pET-28b(+). The sense primer is 5′-AGTTG**CATATG**GTGGTGAGCCCTG-CCG-3′ and the antisense primer is 5′-GATCTT**CTCGAG**TCA-GCGCCACGCGTCGG-3′. The PCR product was digested with the restriction enzymes *Nde*I and *Xho*I (New England Biolabs, Ipswich, Massachusetts, USA) and ligated into pET-28b(+) (Novagen) using the Roche ligation kit to dephosphorylate vector ends before ligating with T4 ligase (Invitrogen). Proper insertion of the *cysQ* gene was confirmed by sequencing.

2.2. Overexpression

The pET-28b(+) *cysQ* construct was transformed into *Escherichia coli* BL21 (DE3). Cells were grown in LB medium supplemented with 30 µg ml^{-1} kanamycin in shaker flasks at 37°C and 220 rev min^{-1}. When the cells reached a density of $OD_{600} \geq 0.5$, protein production was induced with 150 µ*M* isopropyl *β*-D-1-thiogalactopyranoside (IPTG). The cells were grown for 20 h at 18°C and 220 rev min^{-1}. Early test expressions to explore induction conditions used SDS–PAGE and Western blots to confirm His-tagged protein production. Proteins were run on 20% homogeneous PhastGels (GE Healthcare) and transferred to Immbilon-P transfer membrane (Millipore). Anti-His primary antibodies (NeuroMab, Davis, California, USA), goat anti-mouse HRP secondary antibodies (Promega) and TMB Stabilized Substrate (Promega) were used to visualize the Western blots. The cells were harvested by centrifugation at 5000*g* for 10 min at 4°C. The pellet was resuspended in lysis buffer (30 m*M* imidazole, 50 m*M* sodium phosphate pH 8, 800 m*M* sodium chloride) and lysed by passage through a microfluidizer three times. The lysate was cleared by centrifugation at 30 000*g* for 40 min at 4°C.

2.3. Purification

Cleared cell lysate was loaded onto Ni^{2+}–NTA resin (Sigma) pre-equilibrated with lysis buffer. The column was washed with 100 column volumes of lysis buffer overnight. CysQ protein was eluted with a linear gradient of 30–250 m*M* imidazole using elution buffer (250 m*M* imidazole, 300 m*M* sodium chloride, 50 m*M* sodium phosphate pH 8). Protein fractions were identified by absorbance at 280 nm and protein purity was analyzed by SDS–PAGE stained with Coomassie Brilliant Blue. Pure CysQ fractions were pooled and dialyzed overnight against 400 m*M* sodium chloride, 50 m*M* Tris pH 8, 1 m*M* DTT, 5% glycerol.

2.4. Crystallization and data collection

For crystallization, CysQ was concentrated in an Amicon 10K MWCO spin concentrator (Millipore) and buffer-exchanged three times with 20 m*M* Tris pH 8, 100 m*M* sodium chloride, 1 m*M* DTT,

Table 1
Data-collection and processing statistics.

Values in parentheses are for the highest resolution shell.

X-ray source	Beamline 7-1, SSRL
Wavelength (Å)	1.12709
Space group	$P2_12_12_1$
Unit-cell parameters (Å)	a = 40.3, b = 57.9, c = 101.7
Resolution range (Å)	101.7–1.70 (1.74–1.70)
No. of observed reflections	83741 (4351)
No. of unique reflections	26264 (1807)
Completeness (%)	97.3 (92.7)
$\langle I/\sigma(I)\rangle$	13.46 (2.60)
$R_{\rm merge}$† (%)	6.1 (40.1)
Monomers per asymmetric unit	1
Matthews coefficient (Å^3 Da^{-1})	1.95
Solvent content (%)	37

† $R_{\rm merge} = \sum_{hkl}\sum_i |I_i(hkl) - \langle I(hkl)\rangle| / \sum_{hkl}\sum_i I_i(hkl)$, where $\langle I(hkl)\rangle$ is the mean of i observations of reflection hkl.

5% glycerol, 1 m*M* AMP. The final protein concentration was 10 mg ml^{-1} and was used directly in sitting-drop vapor-diffusion crystallization trays. Crystallization conditions were found using the commercially available Microlytic crystallization screens MCSG 1 and MCSG 2 (Burlington, Massachusetts, USA). Crystals grew at room temperature (21°C) in droplets consisting of 1 µl 10 mg ml^{-1} CysQ and 1 µl reservoir solution. To confirm CysQ crystallization, crystals were dissolved in SDS loading dye and analyzed by SDS–PAGE and Western blot (Fig. 2). The crystal that diffracted to the highest resolution grew in 24% PEG 1500, 20% glycerol over 5 d. This crystal (~200 µm) was flash-cooled in liquid nitrogen directly from the crystallization drop. Diffraction data were collected on beamline 7-1 at the Stanford Synchrotron Radiation Lightsource (SSRL). A complete data set was collected to 1.7 Å resolution using beam slits of 100 × 100 µm with a $\Delta\varphi$ of 0.3° and an exposure time of 10 s. Table 1 lists the data-processing statistics.

3. Results and discussion

The *cysQ* gene from *M. tuberculosis* H37Rv codes for a protein of 267 residues with a molar mass of 28.4 kDa. The *cysQ* gene was successfully cloned into pET-28b(+) expression vector and over-expressed in *E. coli* BL21 (DE3) cells, which added 21 residues including a His tag at the N-terminus (MGSSHHHHHH-SSGLVPRGSHM), corresponding to a final protein molecular weight of 30.7 kDa. Test expressions in *E. coli* BL21 (DE3) cells were conducted, varying the induction temperature between 37 and 15°C, and protein bands were identified by SDS–PAGE and confirmed by Western blot. Moderate CysQ yields were observed at 37°C after 2.5 h of induction; however, significant protein contamination was observed. Contaminating proteins were mostly smaller than CysQ when analyzed by SDS–PAGE (not shown). When induction was carried out at 15°C, CysQ yields were reduced but contaminating proteins larger than CysQ were observed.

The protein was purified using Ni^{2+}–NTA resin (Sigma). However, following the manufacturer's protocol of 500 m*M* NaCl in the lysis and wash buffers and washing the column with six to eight column volumes of wash buffer resulted in impure protein as analyzed by SDS–PAGE. We found that increasing the salt concentration to 800 m*M* NaCl and washing the column extensively with 100 column volumes of buffer overnight removed the impurities, resulting in pure protein as analyzed by Coomassie-stained SDS–PAGE (Fig. 2). The CysQ protein ran anomalously low, but the plasmid sequence confirmed the full-length gene and Western blot analysis confirmed the presence of the His tag in the expressed protein (Fig. 2). The protein required no further purification steps and was dialyzed and concentrated after elution from the Ni^{2+}–NTA column for crystallization trials. The best yields of CysQ were purified from cells induced at 18°C for 20 h; typical yields are 0.4–0.8 mg of pure protein per litre of culture.

Initial CysQ crystal screening comprised 192 crystallization conditions using two commercially available 96-well format crystallization screens. CysQ crystallized in a number of conditions over the course of 5 d at 21°C. The best diffracting crystals came from 24% PEG 1500, 20% glycerol with no buffer in the mother liquor (Fig. 3). We confirmed the CysQ protein content of the crystals by Coomassie-stained SDS–PAGE and Western blot analysis of dissolved crystals (Fig. 2).

Crystals were flash-cooled directly from mother liquor by mounting them in loops and plunging them into liquid nitrogen for data collection. Diffraction data were collected on beamline 7-1 of the SSRL. The best diffracting crystals exhibited macroscopic twinning with multiple distinct diffraction lattices (Fig. 4), which was not surprising given a crystal morphology that appeared to contain satellite crystal protrusions (Fig. 3). Fortunately, the software was able to single out and index one lattice, and a data-collection strategy

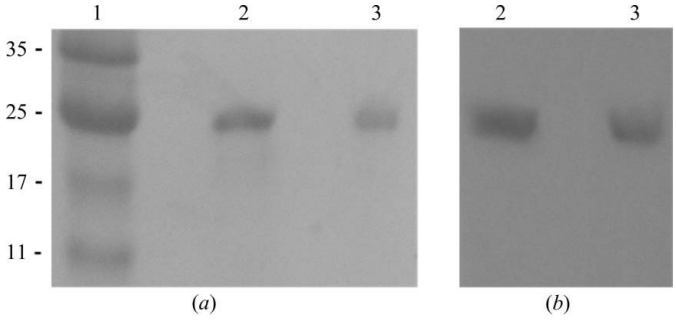

Figure 2
SDS–PAGE analysis of purified protein after buffer exchange and crystallization. (*a*) SDS–PAGE gel stained with Coomassie Blue. Lane 1, molecular-weight markers (labeled in kDa); lane 2, CysQ (~1 mg ml^{-1}) after purification and buffer exchange prior to crystallization; lane 3, crystals dissolved in SDS loading dye. All samples were boiled for 5 min before loading onto a 20% homogeneous polyacrylamide gel. (*b*) Western blot of the gel. Before the gel was stained with Coomassie Blue, the protein was partially transferred to a Western blot membrane. Anti-His-tag antibodies were used to confirm that the crystallized protein band contained the 6×histidine tag. The lanes are the same as in (*a*).

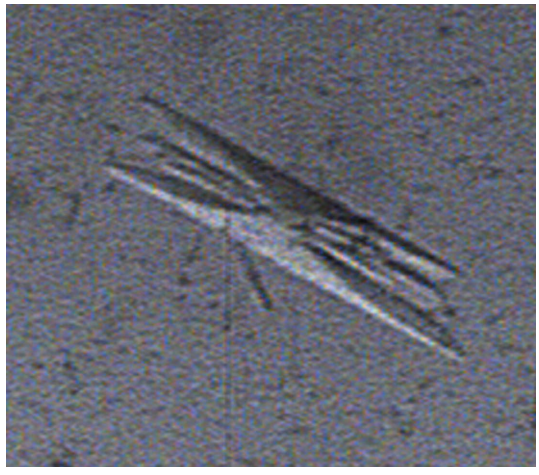

Figure 3
Crystal of CysQ grown in 24% PEG 1500, 20% glycerol using sitting-drop diffusion. The protein sample was in 20 m*M* Tris pH 8, 100 m*M* sodium chloride, 5% glycerol, 1 m*M* DTT, 1 m*M* AMP. The longest crystal dimension is about 200 µm.

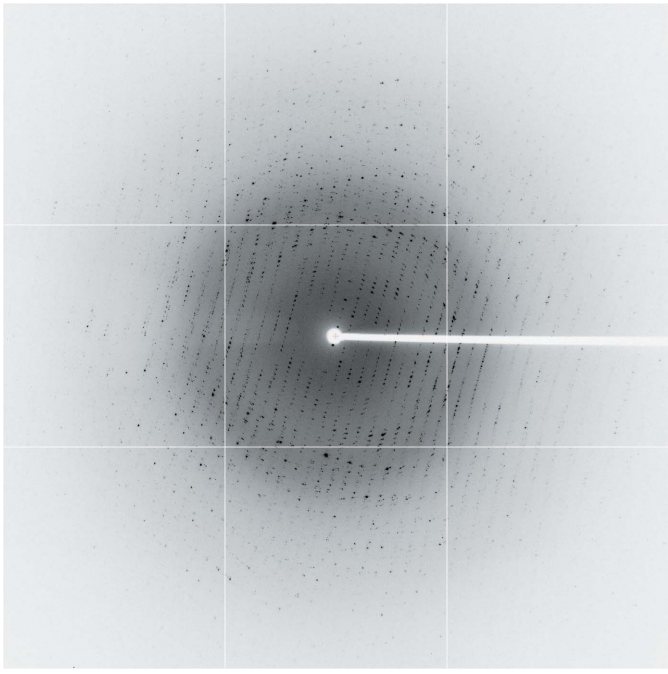

Figure 4
Diffraction pattern of CysQ collected on beamline 7-1 at the Stanford Synchrotron Radiation Laboratory (SSRL) using an ADSC Quantum Q315 CCD detector. The exposure time was 10 s with an oscillation angle of 0.3°. The beam size was 100 × 100 µm.

was computed. A data set was collected using the fine-φ technique with an oscillation angle of 0.3°. Data were processed with *XDS* and scaled with *XSCALE* (Kabsch, 2010*a*,*b*). A 97% complete data set was collected to 1.7 Å resolution with an overall $R_{\rm merge}$ of 6.1% (Table 1).

CysQ crystallized in the orthorhombic point group 222, with unit-cell parameters a = 40.3, b = 57.9, c = 101.7 Å. Inspection of the systematic absences suggested space group $P2_12_12_1$. The Matthews coefficient $V_{\rm M}$ was calculated to be 1.95 Å^3 Da^{-1}, resulting in a solvent content of 37% assuming one monomer per asymmetric unit (Matthews, 1968).

Attempts at molecular replacement were unsuccessful using the closest known structural homologue inositol monophosphatase II from *Staphylococcus aureus* (PDB entry 3t0j; A. Dutta, S. Bhattacharyya, D. Dutta & A. K. Das, unpublished work), which exhibits 25% sequence identity over 199 residues. Therefore, selenomethionine-labeled CysQ protein, which contains five methionines, will be generated to determine the structure using SeMet multiwavelength anomalous dispersion techniques.

AIE was supported in part by the NIH training grant T32-GM007377. Portions of this research were carried out at the Stanford Synchrotron Radiation Lightsource, a Directorate of SLAC National Accelerator Laboratory and an Office of Science User Facility operated for the US Department of Energy Office of Science by Stanford University. The SSRL Structural Molecular Biology Program is supported by the DOE Office of Biological and Environmental Research and by the National Institutes of Health, National Institute of General Medical Sciences (including P41GM103393). The contents of this publication are solely the responsibility of the authors and do not necessarily represent the official views of NIGMS or NIH.

References

Fauci, A. S. (2008). *J. Infect. Dis.* **197**, 1493–1498.
Goren, M. B., Brokl, O. & Schaefer, W. B. (1974). *Infect. Immun.* **9**, 142–149.
Hatzios, S. K., Iavarone, A. T. & Bertozzi, C. R. (2008). *Biochemistry*, **47**, 5823–5831.
Hatzios, S. K., Schelle, M. W., Newton, G. L., Sogi, K. M., Holsclaw, C. M., Fahey, R. C. & Bertozzi, C. R. (2011). *Bioorg. Med. Chem. Lett.* **21**, 4956–4959.
Kabsch, W. (2010*a*). *Acta Cryst.* D**66**, 125–132.
Kabsch, W. (2010*b*). *Acta Cryst.* D**66**, 133–144.
Matthews, B. W. (1968). *J. Mol. Biol.* **33**, 491–497.
Mougous, J. D., Green, R. E., Williams, S. J., Brenner, S. E. & Bertozzi, C. R. (2002). *Chem. Biol.* **9**, 767–776.
Paritala, H. & Carroll, K. S. (2013). *Infect. Disord. Drug Targets*, **13**, 85–115.
Pi, N., Hoang, M. B., Gao, H., Mougous, J. D., Bertozzi, C. R. & Leary, J. A. (2005). *Anal. Biochem.* **341**, 94–104.
Pinto, R., Tang, Q. X., Britton, W. J., Leyh, T. S. & Triccas, J. A. (2004). *Microbiology*, **150**, 1681–1686.
Sassetti, C. M., Boyd, D. H. & Rubin, E. J. (2001). *Proc. Natl Acad. Sci. USA*, **98**, 12712–12717.
Sassetti, C. M., Boyd, D. H. & Rubin, E. J. (2003). *Mol. Microbiol.* **48**, 77–84.
Sekowska, A., Kung, H.-F. & Danchin, A. (2000). *J. Mol. Microbiol. Biotechnol.* **2**, 145–177.
World Health Organization (2013). *Global Tuberculosis Report 2013*. Geneva: World Health Organization. http://www.who.int/tb/publications/global_report/en/.